Interference between resonant and Auger mechanisms for charge-exchange processes near surfaces

Evelina A. García,* N. P. Wang,† and R. C. Monreal
Department Física Teórica de la Materia Condensada, C-V, Universidad Autónoma de Madrid, E-28049 Madrid, Spain

E. C. Goldberg
Instituto de Desarrollo Tecnológico para la Industria Química (CONICET-UNL), Güemes 3450, CC91, 3000, Santa Fe, Argentina
(Received 27 November 2002; published 30 May 2003)

In this work we solve the dynamics of the Newns-Anderson Hamiltonian supplemented with Auger terms and analyze the case of He^+ scattered off an Al (100) surface. The dynamical solution is compared with results of calculations based on much simpler approximations. We prove that resonant and Auger processes can be treated separately and independently in this case and that charge exchange between He and Al proceeds via resonant and Auger exchange of electrons between the promoted molecular orbital of He and the conduction band states of Al.

DOI: 10.1103/PhysRevB.67.205426 PACS number(s): 79.20.Rf, 34.50.Fa

I. INTRODUCTION

Ion surface collisions have long been used as a tool for surface analysis. The collision determines the final charge of the different ionic species, the amount of electron emission, and the sputtered particles from the solid. The collision process is a dynamical situation in which charge exchange between ion and solid evolve in time. Resonant and Auger mechanisms are responsible for this charge exchange. Resonant processes are basically one-electron, tunneling processes between conduction band states of the solid and high lying levels of the atom. In contrast, Auger processes involve at least two electrons and then a many-body description is necessary, especially when plasmon-assisted neutralization is important. Then, while the dynamical quantum-mechanical aspects of resonant charge exchange processes have been analyzed by many authors,[1–9] Auger processes have mostly been treated within a semiclassical approximation (SCA).[10] The purpose of this paper is to include resonant and Auger processes into an unified model for ion neutralization. Our model Hamiltonian is the usual Newns-Anderson Hamiltonian which describes resonant processes, supplemented with terms describing Auger processes (NAA Hamiltonian). In the trajectory approximation, the Hamiltonian depends on time through the dependence of its matrix elements on the distance between atom and surface and the quantum, time dependent problem is solved by means of the Keldysh formalism.[11] A similar problem was addressed in Ref. 12, where the Green's function for the atomic state proposed by Keldysh was obtained through its equations of motion and the self-energies calculated up to second order in the interaction terms. In this work, however, accuracy in the description of the actual process was sacrificed on behalf of simplicity and thus several of the approximations made led to too large values of some interactions. In the present work we perform realistic calculations for the case study of He^+ on Al and the results of the dynamical calculations are compared with results of calculation based on much simpler approximations. An interesting question addressed in Refs. 4,5 is when the SCA is a good approximation to the full dynamical solution. In the SCA one first solves a static problem and gets the energy position and width of the atomic level; then the rates for capture and loss processes are obtained fron these widths as a function of the distance between atom and surface. The rates are then inserted into a classical master equation which allows us to obtain the occupancy of the atomic level as a function of time.[13,14] In Sec. II we obtain an approximate static solution of the NAA Hamiltonian and see that close enough to the surface the hybridization between the orbitals of atom and solid is so strong that it is not possible to especify magnitudes such as energy and width of the atomic level at these distances. In Sec. III we solve for the time evolution of our model Hamiltonian. The solution will be compared with results of the SCA and we will answer the important question of whether Auger and resonant processes should be treated coherently or independently. Simplified calculations presented in Ref. 12 suggested that quantum interferences between Auger and resonant processes can have important consequences in the calculation of atomic occupancies. Our calculations show that this is not indeed the case for He^+ on Al and from this result we can infer that resonant and Auger processes should interfere seldom. In this section we will also show by explicit calculations that charge transfer between He and Al takes place between a promoted molecular orbital (MO) and the conduction band states of Al. Our conclusions are presented in Sec. IV. Atomic units ($e=\hbar=m=1$) are used throughout this work.

II. NAA HAMILTONIAN AND STATIC SOLUTION

Our model Hamiltonian is the spinless Newns-Anderson Hamiltonian supplemented with terms describing Auger processes and reads

$$\hat{H}=\tilde{E}_a(\mathbf{R})\hat{n}_a+\sum_{\mathbf{k}}\epsilon_{\mathbf{k}}\hat{n}_{\mathbf{k}}+\sum_{l}\epsilon_l\hat{n}_l+\sum_{\mathbf{k}}[T_{a,\mathbf{k}}(\mathbf{R})\hat{c}_a^{\dagger}\hat{c}_{\mathbf{k}}+\text{H.c.}]+\sum_{l}[T_{a,l}(\mathbf{R})\hat{c}_a^{\dagger}\hat{c}_l+\text{H.c.}]+\sum_{\mathbf{k}\neq\mathbf{k}'\neq\mathbf{k}'',\sigma'}[V^A_{\mathbf{k},\mathbf{k}'\sigma',\mathbf{k}''\sigma',a}(\mathbf{R})\hat{c}_{\mathbf{k}}^{\dagger}\hat{c}_{\mathbf{k}'\sigma'}^{\dagger}\hat{c}_{\mathbf{k}''\sigma'}\hat{c}_a+\text{H.c.}]. \quad (1)$$

In Eq. (1) $\tilde{E}_a$ is the ''diabatic'' atomic energy level, $\mathbf{R}$ is the position of the atom with respect to the surface, $\epsilon_{\mathbf{k}}$ and ϵ_l are the energies of the metal conduction band states and localized states, respectively, $T_{a,\mathbf{k}}$ and $T_{a,l}$ being their respective hopping integrals with the atomic orbital. The last term in Eq. (1) describes Auger processes with matrix elements

$$V^A_{\mathbf{k},\mathbf{k}'\sigma',\mathbf{k}''\sigma',a}(\mathbf{R}) = \int d\mathbf{r}_1 \int d\mathbf{r}_2 \phi^*_{\mathbf{k}}(\mathbf{r}_1)\phi^*_{\mathbf{k}'}(\mathbf{r}_2) \times V_{\text{screen}}(\mathbf{r}_1,\mathbf{r}_2)\phi_{\mathbf{k}''}(\mathbf{r}_2)\phi_a(\mathbf{r}_1), \quad (2)$$

where $V_{\text{screen}}(\mathbf{r}_1,\mathbf{r}_2)$ is the Coulomb potential appropriately screened, $\phi_{\mathbf{k}}$, $\phi_{\mathbf{k}'}$, and $\phi_{\mathbf{k}''}$ are the wave functions for the conduction band states $|\mathbf{k}\rangle$, $|\mathbf{k}'\rangle$, and $|\mathbf{k}''\rangle$, respectively, and ϕ_a is the wave function of the atomic orbital. It should be kept in mind that states $|\mathbf{k}\rangle$, $|\mathbf{k}'\rangle$, and $|\mathbf{k}''\rangle$ have to be all different since we are describing a process in which a metal electron is transferred to the ion with simultaneous excitation of another metal electron.

Different methods can be used to obtain adiabatic atomic levels interacting with a continuum of states.[15–18] Here, the energy position and width of the adiabatic level are obtained from the resonances of the spectral density of states defined as[19]

$$\rho_a(\omega) = -\frac{1}{\pi}\text{Im}\langle\langle \hat{c}_a ; \hat{c}^\dagger_a\rangle\rangle(\omega + i\eta), \quad (3)$$

where η is an infinitesimal, Im stands for the imaginary part, and $\langle\langle \hat{c}_a ; \hat{c}^\dagger_a\rangle\rangle(\omega)$ is the Fourier transform of the retarded two-times Green's function

$$\langle\langle \hat{c}_a(t); \hat{c}^\dagger_a(t')\rangle\rangle = -i\theta(t-t')\langle \hat{c}^\dagger_a(t')\hat{c}_a(t) + \hat{c}_a(t)\hat{c}^\dagger_a(t')\rangle, \quad (4)$$

with the definition,

$$\langle\langle \hat{c}_a ; \hat{c}^\dagger_a\rangle\rangle(\omega) = \int_{-\infty}^{+\infty} d(t-t')\langle\langle \hat{c}_a(t); \hat{c}^\dagger_a(t')\rangle\rangle e^{i\omega(t-t')}. \quad (5)$$

This Green's function can be obtained exactly if only one-electron interaction terms appear in the Hamiltonian but this is not the case in the presence of Auger terms due to the multielectron character of the Auger interaction. A convenient way of obtaining an approximate expression for $\langle\langle \hat{c}_a ; \hat{c}^\dagger_a\rangle\rangle$ is provided by the method of the equations of motion. Following this method, we first take the derivative of Eq. (4) with respect to *t*. Then, making use of the relation

$$\frac{d\hat{O}}{dt} = i[\hat{H}, \hat{O}],$$

valid for any operator $\hat{O}$ and Fourier-transforming in time we obtain

$$\begin{aligned}(\omega - \tilde{E}_a)\langle\langle \hat{c}_a ; \hat{c}^\dagger_a\rangle\rangle(\omega) &= 1 + \sum_{\mathbf{k}} T^*_{a,\mathbf{k}}\langle\langle \hat{c}_{\mathbf{k}} ; \hat{c}^\dagger_a\rangle\rangle(\omega) + \sum_l T^*_{a,l}\langle\langle \hat{c}_l ; \hat{c}^\dagger_a\rangle\rangle(\omega) \\ &+ \sum_{\mathbf{k}\neq\mathbf{k}'\neq\mathbf{k}'',\sigma'} V^A_{\mathbf{k},\mathbf{k}'\sigma',\mathbf{k}''\sigma',a}\langle\langle \hat{c}^\dagger_{\mathbf{k}''\sigma'}\hat{c}_{\mathbf{k}'\sigma'}\hat{c}_{\mathbf{k}} ; \hat{c}^\dagger_a\rangle\rangle(\omega). \end{aligned} \quad (6)$$

The next step is to calculate the new Green's functions appearing on the right-hand side of Eq. (6) from their equations of motion and then keep terms to lowest order in the interaction integrals T and V^A. In this way we can approximate

$$(\omega - \epsilon_{\mathbf{k}})\langle\langle \hat{c}_{\mathbf{k}} ; \hat{c}^\dagger_a\rangle\rangle(\omega) \simeq T_{a,\mathbf{k}}\langle\langle \hat{c}_a ; \hat{c}^\dagger_a\rangle\rangle(\omega) \quad (7)$$

and

$$(\omega - \epsilon_l)\langle\langle \hat{c}_l ; \hat{c}^\dagger_a\rangle\rangle(\omega) \simeq T_{a,l}\langle\langle \hat{c}_a ; \hat{c}^\dagger_a\rangle\rangle(\omega). \quad (8)$$

For the fourth term of Eq. (6) and neglecting exchange terms, we obtain after a lengthy calculation

$$\begin{aligned}(\omega + \epsilon_{\mathbf{k}''} - \epsilon_{\mathbf{k}'} - \epsilon_{\mathbf{k}})\langle\langle \hat{c}^\dagger_{\mathbf{k}''\sigma'}\hat{c}_{\mathbf{k}'\sigma'}\hat{c}_{\mathbf{k}} ; \hat{c}^\dagger_a\rangle\rangle(\omega) &\simeq \langle\langle \hat{c}_a ; \hat{c}^\dagger_a\rangle\rangle(\omega)[\langle 1-\hat{n}_{\mathbf{k}''}\rangle\langle\hat{n}_{\mathbf{k}'}\rangle\langle\hat{n}_{\mathbf{k}}\rangle V^A_{\mathbf{k},\mathbf{k}'\sigma',\mathbf{k}''\sigma',a} \\ &+ \langle\hat{n}_{\mathbf{k}''}\rangle\langle 1-\hat{n}_{\mathbf{k}'}\rangle\langle 1-\hat{n}_{\mathbf{k}}\rangle V^A_{\mathbf{k},\mathbf{k}'\sigma',\mathbf{k}''\sigma',a}], \end{aligned} \quad (9)$$

where, to zeroth order in the interaction integrals, $\langle\hat{n}_{\mathbf{k}}\rangle$ is the Fermi-Dirac function evaluated at the energy $\epsilon_{\mathbf{k}}$. As we will see below, the second and third terms on the right-hand side of Eq. (9) describe Auger capture and Auger loss processes, respectively.

Equations (7) and (8) and (9) are now inserted in Eq. (6) and our final expression for the spectral density of states reads

$$\rho_a(\omega) = -\frac{1}{\pi}\text{Im}\frac{1}{\omega - \tilde{E}_a - \Sigma_R(\omega + i\eta) - \Sigma_A(\omega + i\eta)}, \quad (10)$$

where $\Sigma_R(\omega + i\eta)$ and $\Sigma_A(\omega + i\eta)$, the self-energies for resonant and Auger processes respectively, are given by

$$\Sigma_R(\omega + i\eta) = \sum_{\mathbf{k}} \frac{|T_{a,\mathbf{k}}|^2}{\omega - \epsilon_{\mathbf{k}} + i\eta} + \sum_l \frac{|T_{a,l}|^2}{\omega - \epsilon_l + i\eta} \quad (11)$$

and

$$\Sigma_A(\omega + i\eta) = \Sigma_{\text{AC}}(\omega + i\eta) + \Sigma_{\text{AL}}(\omega + i\eta), \quad (12)$$

where the self-energies for Auger capture and Auger loss processes read

$$\Sigma_{\text{AC}}(\omega + i\eta) = \sum_{\mathbf{k},\mathbf{k}',\mathbf{k}'',\sigma'} \frac{|V^A_{\mathbf{k},\mathbf{k}'\sigma',\mathbf{k}''\sigma',a}|^2}{\omega + \epsilon_{\mathbf{k}''} - \epsilon_{\mathbf{k}'} - \epsilon_{\mathbf{k}} + i\eta}\langle 1-\hat{n}_{\mathbf{k}''}\rangle \times \langle\hat{n}_{\mathbf{k}'}\rangle\langle\hat{n}_{\mathbf{k}}\rangle, \quad (13)$$

and

$$\Sigma_{\mathrm{AL}}(\omega+i\eta)=\sum_{\mathbf{k},\mathbf{k}',\mathbf{k}'',\sigma'}\frac{|V^{A}_{\mathbf{k},\mathbf{k}'\sigma',\mathbf{k}''\sigma',a}|^2}{\omega+\epsilon_{\mathbf{k}''}-\epsilon_{\mathbf{k}'}-\epsilon_{\mathbf{k}}+i\eta}\times\langle\hat{n}_{\mathbf{k}''}\rangle\langle 1-\hat{n}_{\mathbf{k}'}\rangle\langle 1-\hat{n}_{\mathbf{k}}\rangle. \tag{14}$$

In the jellium model, Eqs. (13) and (14) can be expressed in terms of the matrix elements for the transition of one metal electron to/from the atomic state $M_{a,\mathbf{k}}$ and the dynamical susceptibility for interacting electrons $\chi(q,\omega;z,z')$. Following the steps of Ref. 20, our final expression for the Auger self-energies are

$$\Sigma_{\mathrm{AC}}(\omega+i\eta)=\frac{1}{\pi}\sum_{\mathbf{k}<k_F}\int_0^\infty\frac{d\omega'}{\omega-\epsilon_{\mathbf{k}}+\omega'+i\eta}\int\frac{d^2\mathbf{q}}{(2\pi)^2}\times\int dz\int dz'-\mathrm{Im}\,\chi(q,\omega;z,z')\times M^{*}_{a,\mathbf{k}}(\mathbf{q},z)M_{a,\mathbf{k}}(\mathbf{q},z') \tag{15}$$

and

$$\Sigma_{\mathrm{AL}}(\omega+i\eta)=\frac{1}{\pi}\sum_{\mathbf{k}>k_F}\int_0^\infty\frac{d\omega'}{\omega-\epsilon_{\mathbf{k}}-\omega'+i\eta}\int\frac{d^2\mathbf{q}}{(2\pi)^2}\times\int dz\int dz'-\mathrm{Im}\,\chi(q,\omega;z,z')\times M^{*}_{a,\mathbf{k}}(\mathbf{q},z)M_{a,\mathbf{k}}(\mathbf{q},z'), \tag{16}$$

where k_F is the Fermi wave vector and $M_{a,\mathbf{k}}$ is given by

$$M_{a,\mathbf{k}}(\mathbf{q},z)=\frac{2\pi}{q}\langle\phi_{\mathbf{k}}|e^{i\mathbf{q}\cdot\mathbf{x}_1}e^{-q|z-z_1|}|\phi_a\rangle. \tag{17}$$

When calculating the resonant self-energy, we follow the linear combination of atomic orbitals (LCAO) approach used in Refs. 21,22 and write down metal Bloch states in terms of different atomic orbitals. Assuming that core orbitals give rise to completely flat bands, the resonant self-energy can be written as

$$\Sigma_R(\omega+i\eta)=\sum_{i,j}T_{i,a}T_{j,a}\int d\epsilon\frac{\rho_{ij}(\epsilon)}{\omega-\epsilon+i\eta}+\sum_l\frac{|T_{l,a}|^2}{\omega-\epsilon_l+i\eta}, \tag{18}$$

where i,j denote the conduction bands orbitals and $\rho_{ij}(\epsilon)$ the corresponding density of states. For the case of He on Al, $\tilde{E}_a$, $T_{i,a}$, and $T_{l,a}$ were calculated in Ref. 22 as a function of the distance between He and the first atomic layer of Al. The relevant orbitals are He-1s, Al-3s, and 3p for the conduction band orbitals and Al- 2s and 2p as core orbitals. See Figs. 1 and 2 of Ref. 22 for details. For all of these orbitals the Hartree-Fock single-zeta wave functions of Ref. 23 were used and He was assumed to be on-top position.

With respect to the Auger self-energies, it is easy to see that the imaginary part of the Auger self-energies for capture and loss processes, Eqs. (15) and (17) respectively, are related to the golden rule Auger rates $1/\tau_{\mathrm{AC}}$ and $1/\tau_{\mathrm{AL}}$[24] by

$$\mathrm{Im}\,\Sigma_A(\omega+i\eta)=-\frac{1}{2}\left(\frac{1}{\tau_{\mathrm{AC}}}+\frac{1}{\tau_{\mathrm{AL}}}\right)(\omega). \tag{19}$$

The real part of $\Sigma_A(\omega)$ gives the contribution of Auger processes to the energy shift of the atomic level but this contribution is negligible for the case of He on Al that we investigate. Therefore in the calculations we will show below the Auger self-energy has been approximated by its imaginary part Eq. (19). Moreover and for the reasons we will give in the next section, we assume that the Auger capture rate decreases exponentially away from the jellium edge $z_j=2$ a.u., as suggested by explicit calculations shown in Ref. 24,

$$\frac{1}{\tau_{\mathrm{AC}}}(\omega)=\frac{1}{\tau^{b}_{\mathrm{AC}}}(\omega)\times\begin{cases}e^{-(z-z_j)/d}\ \text{if}\ z>z_j,\\ 1\ \text{if}\ z<z_j,\end{cases} \tag{20}$$

where the saturation value $(1/\tau^{b}_{\mathrm{AC}})(\omega)$ is calculated using the bulk formula for the Auger transition rates[25] in order to include the plasmon assisted neutralization processes.[26] However, the value of the decay length d is the one obtained using a surface response function, $d=1.15$ a.u. from Ref. 21. With respect to the Auger loss processes, notice that these processes only can occur in the static case when the atomic energy level is above the Fermi level and this means distances shorter than z_j for He on Al. Therefore, in our approximation $1/\tau_{\mathrm{AL}}$ is calculated in bulk[25] and is independent of distance.

The spectral density of states calculated in this way is shown in Fig. 1 for distances between He and the first atomic layer of Al of (a) 2 a.u., (b) 1 a.u., and (c) 0.9 a.u. In Fig. 1(a), the resonant interaction between He and the conduction band orbitals of Al shifts down the energy level of He (note the appearance of a small weight in the density of states near the top of the conduction band) but since the peak position is below the bottom of the conduction band and there is little weight at the energies of the conduction band states, the level width is only due to Auger capture and the line shape is Lorentzian. Up to distances of around 1.1–1.2 a.u. the spectral density of states shows a sharp peak below the bottom of the conduction band even though there is an increase of spectral weight of the energies within the conduction band. We will show in the next section that the SCA is a very good approximation for problems in which He is scattered off Al at distances of the order of 1 a.u. or larger. In Fig. 1(b) the He-1s energy level has been promoted in such a way that the peak position is within the conduction band. Note how the line shape is being distorted with respect to the Lorentzian line shape and how the peak is much wider than in Fig. 1(a). The interaction between He and the core orbitals of Al is mainly responsible for the position of the peak but the width of the level is mostly due to the resonant interaction with the conduction band states. In Fig. 1(c) the hybridization between the atomic orbitals of He and Al is so strong that the spectral density of states is as wide as the conduction band of Al. The same situation is found at shorter distances. In these cases it is impossible to define a level width with confidence and this renders the SCA a very unreliable approximation.

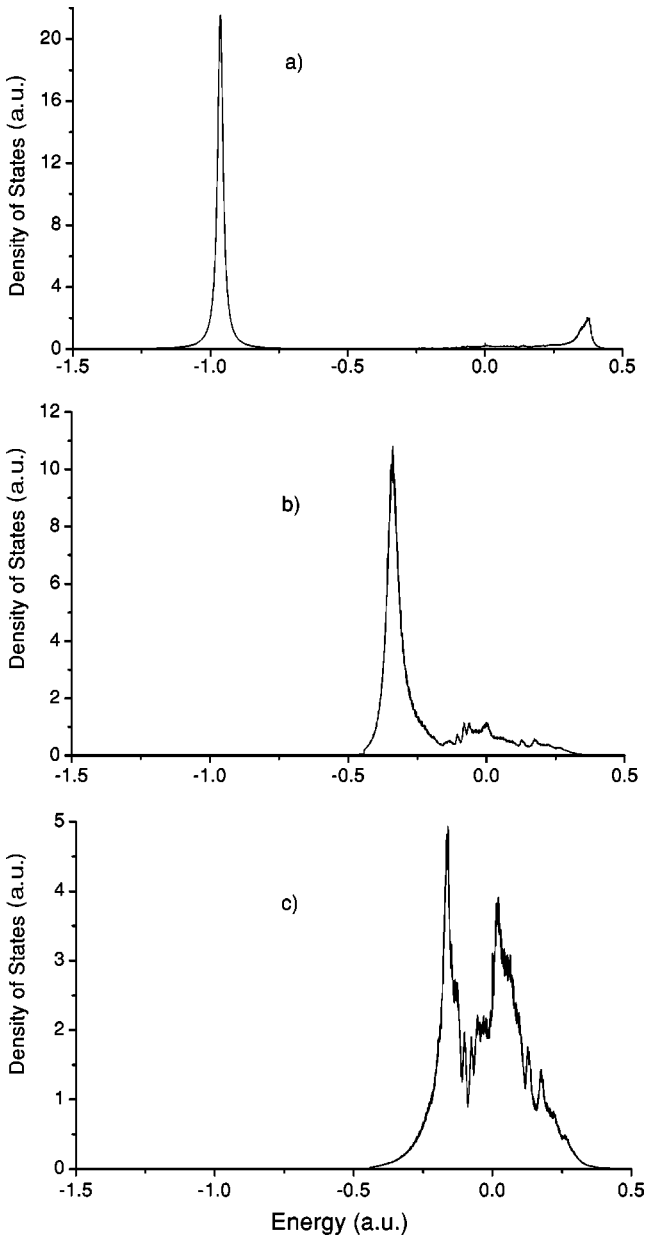

FIG. 1. The spectral density of states as a function of energy for distances between He and the first atomic layer of Al of (a) 2 a.u., (b) 1 a.u., and (c) 0.9 a.u. Energy is referred to the Fermi level. The top and the bottom of the conduction band of Al are at energies of 0.43 and -0.43 a.u., respectively.

Therefore a full dynamical quantum description of charge exchange is necessary whenever He can get closer than 1 a.u. from an Al atom.

III. DYNAMICAL SOLUTION OF THE NAA HAMILTONIAN: RESULTS AND DISCUSSION

In this section, the time-dependent evolution of the occupancy of the He-1*s* level is analyzed using Keldysh Green's function techniques. Details have been published elsewhere.[12,27,28] Let us only summarize here that the basic quantity we need is the two-times retarded self-energy $\Sigma(t,t')$. This quantity can be found using the equations of motion method and, as in the static case, keeping terms to lowest order in the interaction integrals. The result is

$$\Sigma(t,t')=\Sigma_R(t,t')+\Sigma_{\mathrm{AC}}(t,t')+\Sigma_{\mathrm{AL}}(t,t'), \tag{21}$$

where the resonant self-energy is given by

$$\Sigma_R(t,t')=-i\theta(t-t') \times\left[\sum_{i,j} T_{i,a}(t)T_{j,a}(t')\int d\epsilon\rho_{ij}(\epsilon)e^{-i\epsilon(t-t')} +\sum_{l} T_{l,a}(t)T_{l,a}(t')e^{-i\epsilon_l(t-t')}\right], \tag{22}$$

and the self-energies for Auger capture and loss processes are given by

$$\Sigma_{\mathrm{AC}}(t,t')=-i\theta(t-t')\sum_{\mathbf{k}<k_F}\int_0^\infty\frac{d\omega}{\pi}e^{-i(\epsilon_{\mathbf{k}}-\omega)(t-t')} \times\int\frac{d^2\mathbf{q}}{(2\pi)^2}\int dz\int dz'-\mathrm{Im}\,\chi(q,\omega;z,z') \times M^*_{a,\mathbf{k}}(\mathbf{q},z,t)M_{a,\mathbf{k}}(\mathbf{q},z',t') \tag{23}$$

and

$$\Sigma_{\mathrm{AL}}(t,t')=-i\theta(t-t')\sum_{\mathbf{k}>k_F}\int_0^\infty\frac{d\omega}{\pi}e^{-i(\epsilon_{\mathbf{k}}+\omega)(t-t')} \times\int\frac{d^2\mathbf{q}}{(2\pi)^2}\int dz\int dz'-\mathrm{Im}\,\chi(q,\omega;z,z') \times M^*_{a,\mathbf{k}}(\mathbf{q},z,t)M_{a,\mathbf{k}}(\mathbf{q},z',t'). \tag{24}$$

Equations (22), (23), and (24) produce Eqs. (11), (15), and (16), respectively, in the static limit. However, the calculation of the atomic occupancy using Eqs. (23) and (24) in the dynamical case is too demanding because it is necessary to evaluate a eight-dimensional integral for each pair (t,t') with t and t' along the ion trajectory. (We use 50 000 values of t and t' at the lowest velocities). Therefore in this work we will use some approximations to the Auger self-energies that keep the basic physical ingredients of a full calculation. We propose two *Ansätze* for the Auger self-energies. Both use the exact but much more affordable calculation of $\Sigma_A(t,t')$ in the bulk of the metal done in Ref. 28 and assume an exponential decay away from the surface when either t or t' are such that the corresponding perpendicular distance is outside the jellium edge. As we said before, this exponential decay is found approximately in explicit calculations of the Auger transition rates.[24]

In our first *Ansatz* $\Sigma_{\mathrm{AC,AL}}(t,t')$ are written down[28] as

$$\Sigma^{(1)}_{\mathrm{AC}}(t,t') = \begin{cases} \Sigma^{b}_{\mathrm{AC}}(t-t') \ \text{ if } \ |t|<|t_j| \ \text{ and } \ |t'|<|t_j|, \\ -i\dfrac{1}{2}\Delta_{\mathrm{AC}}(t)\,\delta(t-t') \ \text{ if } \ |t|>|t_j| \ \text{ and } \ |t'|>|t_j|, \\ 0 \ \text{ in other cases} \end{cases} \tag{25}$$

and

$$\Sigma^{(1)}_{\mathrm{AL}}(t,t') = \begin{cases} \Sigma^{b}_{\mathrm{AL}}(t-t') \ \text{ if } \ |t|<|t_j| \ \text{ and } \ |t'|<|t_j|, \\ 0 \ \text{ in other cases.} \end{cases} \tag{26}$$

In Eqs. (25) and (26), $\Sigma^{b}_{\mathrm{AC,AL}}(t-t')$ are the exact bulk self-energies, $\Delta_{\mathrm{AC}}(t)$ is the static full width at half maximum (FWHM) of the peak in the static density of states calculated in Sec. II and t_j is the time at which the ion coordinate perpendicular to the surface equals the jellium edge position z_j. This *Ansatz* implies to use the SCA outside the jellium edge and it is justified because in Ref. 28 the SCA was found to be a vey good approximation for describing Auger processes alone. With respect to Auger loss processes, these processes can only take place when the final position of the energy level is above the Fermi level and this is inside the jellium edge in our case: hence Eq. (26). However, by using Eqs. (22), (25), and (26) the quantum dynamical character of resonant and Auger processes is kept and they are allowed to interfere when they can both contribute to the level width and this is inside the jellium edge. This *Ansatz* has the problem that the Auger self-energies are discontinuous functions of t and t' at t_j which leads to discontinuities in the derivative of the atomic occupancy at t_j.[28] To ascertain how serious the problem is we make a second *Ansatz* in which the Auger self-energy has a form similar to the resonant self-energy. We notice in Eq. (22) that $\Sigma_R(t,t')$ is the product of one factor depending on the time difference $t-t'$ and the hopping integrals depending on t and t', these hopping integrals decreasing exponentially with the distance to the surface similar to the matrix elements $M_{a,\mathbf{k}}$ of Eqs. (23) and (24). In our second *Ansatz*, $\Sigma_{\mathrm{AC,AL}}(t,t')$ are writen down as

$$\Sigma^{(2)}_{\mathrm{AC,AL}}(t,t') = \Sigma^{b}_{\mathrm{AC,AL}}(t-t')f(t)f(t'), \tag{27}$$

with

$$f(t) = \begin{cases} e^{-[z(t)-z_j]/2d} \ \text{ if } \ z>z_j, \\ 1 \ \text{ if } \ z<z_j. \end{cases} \tag{28}$$

Notice that the static limit of Eqs. (22), (27), and (28) is given by Eqs. (18), (19), and (20), respectively. Having defined the self-energies, the Keldysh formalism allows us to obtain the atomic occupancy as a function of time $n_a(t) = \langle \hat{n}_a(t) \rangle$, for a given initial condition of incident ions $[n_a(t\to-\infty)=0]$ or incident neutrals $[n_a(t\to-\infty)=1]$.

In our calculations He^+ is assumed to be perpendicularly incident on an Al (100) surface and scattered off an Al atom of the first atomic layer with scattering angles of 180° and 136°. The loss of kinetic energy in the scattering event is taken into account instantaneously: at the turning point of the trajectory the velocity changes abruptly from the incoming value v_{in} to the outgoing value in the laboratory frame v_{out}, $v_{\mathrm{out}}=0.74v_{\mathrm{in}}$ for a scattering angle of 180° and $v_{\mathrm{out}}=0.77v_{\mathrm{in}}$ for a scattering angle of 136°. Turning points were calculated in Ref. 22 as a function of the incident energy. In this work we will focus on the calculation of the ion survival probability defined as $P^+=1-n_a(t\to+\infty)$, for $n_a(t\to-\infty)=0$, which is the magnitude usually measured in low energy ion scattering (LEIS) experiments.

TABLE I. Comparison of the results for P^+ obtained with the SCA and with the full dynamical calculation for He scattered off Al at an scattering angle of 180°, for several values of the incident kinetic energy.

E_{in} (eV)	115	150	185	211	300	450	1000
SCA	0.055	0.080	0.101	0.117	0.166	0.229	0.373
Dynamical	0.062	0.086	0.109	0.125	0.172	0.236	0.374

The first results we present concern the accuracy of the SCA in cases where the width of the atomic energy level is a well defined quantity. This happens in our case at distances larger than around 1 a.u. and the width is mostly due to Auger processes as we saw in Sec. II. Conditions for the validity of the SCA were derived in Refs. 4,5 for resonant processes in the limit of a very wide conduction band (there is no shift of the diabatic level $\tilde{E}_a$ at all) and in Ref. 28 for Auger processes. However, it is not evident what the conditions should be in the present case, where the resonant self-energy actually leads to a very pronounced shift of the atomic energy level and the Auger self-energy basically contributes only to the level width. The SCA applied to the calculation of P^+ gives

$$P^+ = P^+_{A,\mathrm{in}} \cdot P^+_{A,\mathrm{out}}, \tag{29}$$

where $P^+_{A,\mathrm{in}}$ and $P^+_{A,\mathrm{out}}$, the Auger survival probabilities for the incoming and outgoing trajectories, respectively, are calculated as

$$P^+_{A,\mathrm{in}} = \exp\left[-\frac{1}{v_{\mathrm{in},z}} \int_{z_s}^{\infty} dz\, \Delta_{\mathrm{AC}}(z) \right], \tag{30}$$

and a similar expression for $P^+_{A,\mathrm{out}}$. In Eq. (30) $\Delta_{\mathrm{AC}}(z)$ is the FWHM of the peak of the static density of states calculated in Sec. II, $v_{\mathrm{in},z}$ is the component of the velocity perpendicular to the surface and $z_s=1.1$ a.u. to ensure that the level width is well defined at all distances. In the dynamical calculation we also set the turning point of the trajectories to 1.1 a.u. and use the second *Ansatz* when calculating the Auger self-energies because the first *Ansatz* implies to use the SCA in a part of the trajectory already. In Table I we compare the results of the full dynamical calculation of P^+ with the SCA, Eqs. (29),(30), for a scattering angle of 180°. Note that the differences between both calculations are smaller than 10%, this being a strong indication that Auger processes actually take place almost adiabatically to the final atomic energy level obtained from the static calculation.

Next, we will show that the promotion of the He-1*s* level due to the interaction with the core levels of Al is an adia-

batic process at the velocities of concern for this work, smaller than 1.5 keV. This means that one can safely think that charge transfer between He and Al proceeds between the promoted level of He and the conduction band states of Al via resonant or Auger transfer. To assess this point we will compare the results for P^+ of our full dynamical calculation for the NAA Hamiltonian with the results of another dynamical calculation but for an ''l-adiabatic'' Hamiltonian. In the l-adiabatic Hamiltonian, the diabatic energy levels $\tilde{E}_a$ and ϵ_l are substituted for the set of MO resulting from the interactions $T_{l,a}$ among them. It is assumed that only the MO a^*, which is the MO that approaches asymptotically the atomic orbital a, interacts with the conduction band states of the metal. The l-adiabatic Hamiltonian thus reads

$$\hat{H}_{l\text{-}ad}=E_{a^*}(\mathbf{R})\hat{n}_{a^*}+\sum_{\mathbf{k}}\epsilon_{\mathbf{k}}\hat{n}_{\mathbf{k}}+\sum_{\mathbf{k}}[T_{a^*,\mathbf{k}}(\mathbf{R})\hat{c}^{\dagger}_{a^*}\hat{c}_{\mathbf{k}}+\text{H.c.}]$$
$$+\sum_{\mathbf{k}\neq\mathbf{k}'\neq\mathbf{k}'',\sigma'}[V^A_{\mathbf{k},\mathbf{k}'\sigma',\mathbf{k}''\sigma',a^*}(\mathbf{R})\hat{c}^{\dagger}_{\mathbf{k}}\hat{c}^{\dagger}_{\mathbf{k}'\sigma'}\hat{c}_{\mathbf{k}''\sigma'}\hat{c}_{a^*}$$
$$+\text{H.c.}], \tag{31}$$

where the ''l-adiabatic'' matrix elements are related to the ''diabatic'' ones by

$$T_{a^*,\mathbf{k}}(\mathbf{R})=w^a_{a^*}(\mathbf{R})T_{a,\mathbf{k}}(\mathbf{R}) \tag{32}$$

and

$$V^A_{\mathbf{k},\mathbf{k}'\sigma',\mathbf{k}''\sigma',a^*}(\mathbf{R})=w^a_{a^*}(\mathbf{R})V^A_{\mathbf{k},\mathbf{k}'\sigma',\mathbf{k}''\sigma',a}(\mathbf{R}), \tag{33}$$

where $w^a_{a^*}(\mathbf{R})$ is the weight coefficient of the atomic orbital a into the MO a^*. We define the l-adiabatic ion survival probability as $P^+=1-n_{a^*}(t\to+\infty)$, for $n_{a^*}(t\to-\infty)=0$. Both calculations of the ion survival probability should give similar results if the l-adiabatic approximation is a good one because orbitals a and a^* are the same asymptotically. Also we can check the validity of the l-adiabatic approximation for resonant processes only [$V^A=0$ in Hamiltonians (1) and (31)] and for Auger processes only ($T_{a,\mathbf{k}}=T_{a^*,\mathbf{k}}=0$).

Figure 2 compares the results for P^+ of the full dynamical and of the l-adiabatical calculations for a scattering angle of 180°, for resonant processes only (dots), Auger processes [using *Ansatz* (1)] only (lines) and for both kind of processes included in the Hamiltonian (squares). The extreme accuracy of the l-adiabatic approximation to the dynamical problem is noteworthy. We also present in this figure results of the full dynamical calculation using *Ansatz* (2) for the Auger self-energies (triangles) and note that the differences between calculations using both *Ansatze* are not significant. Also note that the results for P^+ taking into account Auger process only do not follow a perfect straight line; for the highest velocities He can reach a distance at which the l-adiabatic level is above the Fermi level where Auger loss processes are possible. The survival probability for resonant processes (dots) shows two minima at incident kinetic energies of 185 and 450 eV. The first of these is a joint effect of the two Al-core orbitals included in the present calculation; this minimum disappears and only one minimum is left at a higher kinetic energy if we include either the $2s$ level or the $2p$ level of Al.

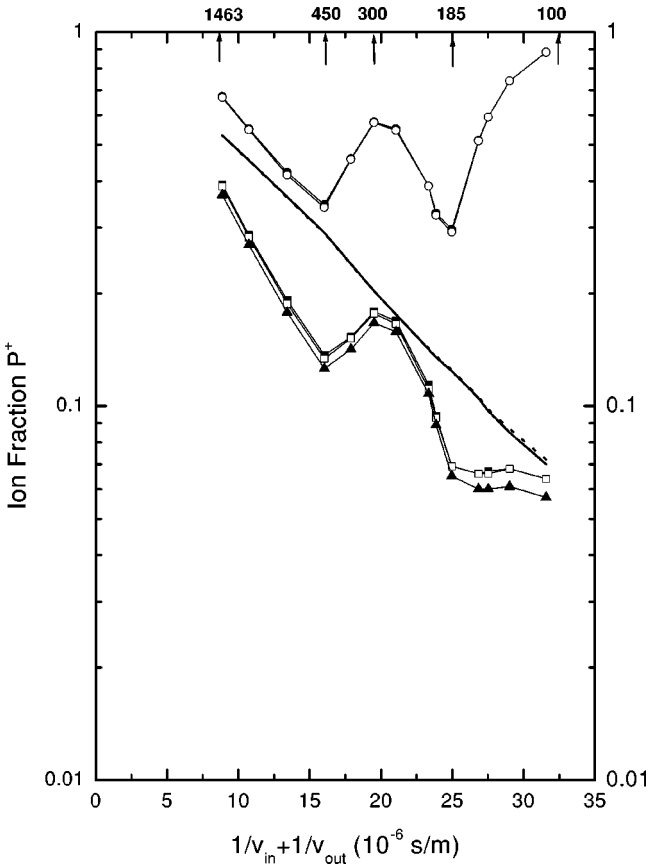

FIG. 2. Comparison of the results for the ion survival probability obtained with the full dynamical calculation (closed symbols) and with the l-adiabatical calculation (open symbols) for the cases of resonant processes only (dots), Auger processes only (lines) and both kinds of processes included in the Hamiltonians (squares). Also shown for comparison are the results of the full dynamical calculation including resonant and Auger processes [*Ansatz* (2)] (triangles). He^+ is scattered from Al at a scattering angle of 180°. Incident kinetic energies (in eV) are marked by arrows on the upper x axis.

An important outcome of the present analysis is to verify that for the case of He on Al Auger and resonant processes can be separated and treated independently. This will be done by comparing the full dynamical solution of the NAA Hamiltonian with the ''separation'' formula[22,29]

$$P^+=P^+_{A,\text{in}}\cdot P^+_{\text{surv}}\cdot P^+_{A,\text{out}}+(1-P^+_{A,\text{in}})\cdot P_{\text{reion}}\cdot P^+_{A,\text{out}}. \tag{34}$$

In this equation $P^+_{A,\text{in}}$ and $P^+_{A,\text{out}}$ are given by Eq. (30) with $z_s=1.1$ a.u. the distance at which the final static energy level crosses the bottom of the conduction band. P^+_{surv} and P_{reion} are the resonant survival probability and the resonant reionization probability, respectively, and both are the results of a dynamical calculation including resonant processes only (that is $V^A=0$ in Hamiltonian (1)] with initial conditions for incident ions and incident neutrals, respectively. Equation

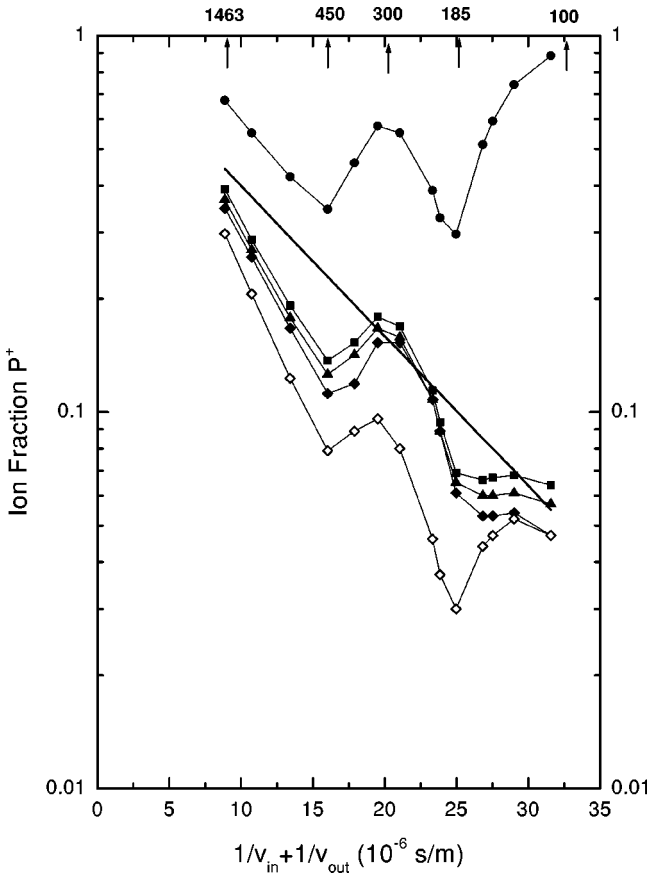

FIG. 3. The contribution of different processes to the ion survival probability of He^+ backscattered from Al at a scattering angle of 180°. Continuous line: Auger survival probability (29). Dots: resonant survival probability. Open diamonds: survival channel. Closed diamonds: P^+ given by the separation approximation, Eq. (34). Closed squares: full dynamical calculation using *Ansatz* (1) for the Auger self-energy. Closed triangles: full dynamical calculation using *Ansatz* (2) for the Auger self-energy. Incident kinetic energies (in eV) are marked by arrows on the upper *x* axis.

(34) implies that Auger and resonant processes can be separated and treated independently.

In Fig. 3 we show, for a scattering angle of 180°, the resonant survival probability $P^+_{\rm surv}$ (dots), the Auger probability of Eq. (29) (continuous line), the probability for the survival channel $P^+_{A,\rm in}P^+_{\rm surv}P^+_{A,\rm out}$ (open diamonds) and the total value of P^+ given by Eq. (34) (solid diamonds). This last result should be compared with the results of the full dynamical calculations with both *Ansätze* for the Auger self-energies represented by solid squares [*Ansatz* (1)] and solid triangles [*Ansatz* (2)]. We can appreciate that the separation approximation is excellent for the ion kinetic energies of the present work. The larger differences between Eq. (34) and the dynamical calculation are in the region of energies smaller than 200 eV, where the resonant channel is opening and in the region of energies around 450 eV, where the resonant channel starts to close. We attribute these differences to quantum interferences between Auger and resonant processes. These results allow us to infer that those interferences should not lead to dramatic effects in a general case. We should expect important quantum-interference effects when we have two processes which can happen at the same time and with similar probabilities. This is going to be very seldom the case with resonant and Auger processes. For the system He/Al, we have just seen that Auger processes contribute to charge tranfer in one part of the trajectory and resonant processes in another, spatially separated part, depending on the position of the atomic energy level relative to the conduction band. For other systems, such as H/Al, the atomic energy level is resonating with the Al conduction band in a large range of distances[13,16] so then resonant and Auger processes could in principle interfere but since we expect that the probability for resonant processes is much larger that the probability for Auger processes [in a way similar to what we find in Figs. 1(a) and 1(b)] we should not expect quantum interferences to play a big role in charge exchange for these systems, either. The calculations for Auger processes, shown as continuous lines in Figs. 2 and 3 differ in that the effect of the resonant interaction with the conduction band states is not included in Fig. 2 (we took $T_{a,\mathbf{k}}=0$ in that calculation).

In Fig. 4 we again compare the results of the full dynamical calculation with the ''separation'' approximation, Eq. (34), for a scattering angle of 136°. The situation is completely similar to the one found in Fig. 4 and the two kind of calculations only differ slightly when the resonant channel opens or closes. The results of this work differ from the calculation presented in Ref. 22 in that we recalculate the Auger survival probabilities according to the level widths found in the static solution of our Hamiltonian, we have included the loss of kinetic energy of He^+ in the scattering event and we have improved the accuracy of the calculation. When comparing the present results with the experimental data, taken for incident energies between 500 and 1000 eV and shown in Ref. 22 we find that the theoretical results for P^+ are a factor of 3 to 5 larger than the experiment. One source of the discrepancy comes from the use of a too simple wave function for He in the calculation of the hopping integrals T and Auger matrix elements V^A. In particular, it was shown in Ref. 30 that the use of a better and more extended wave function increases the values of the rates for Auger capture processes. To see this effect in our dynamical calculations we recalculate the Auger self-energy [*Ansatz* (2)] using the Hartree-Fock wave function of Ref. 31 while leaving the resonant self-energy unchanged. In Fig. 5 we compare the results of both dynamical calculations. The theoretical results improve by 50–100 % in the energy range 500–1000 eV but are still a factor of 2–3 larger than the experiment. This suggest that we can expect further improvement of our calculation if we would recalculate the hopping integrals with a better and more extended description of He and Al orbitals. Also, a more realistic description of the interaction between He and the Al surface, taking into account more than one atom, should lead to different results, especially for the larger incident energies, when the turning points of the trajectories are closer to the surface. Finally, another effect that has to be considered is the fact that the velocity of the projectile do not change abruptly at the turning point of the trajectory but rather the loss of kinetic energy is gradual until

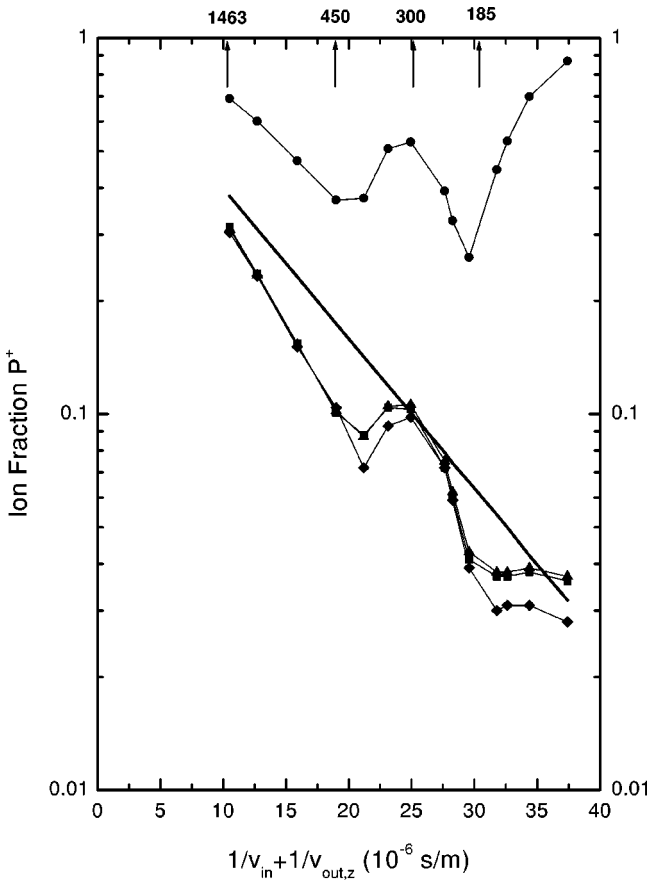

FIG. 4. The contribution of different processes to the ion survival probability of He^+ backscattered from Al at a scattering angle of 136°. Continuous line: Auger survival probability (29). Dots: resonant survival probability. Closed diamonds: P^+ given by the separation approximation (34). Closed squares: full dynamical calculation using *Ansatz* (1) for the Auger self-energy. Closed triangles: full dynamical calculation using *Ansatz* (2) for the Auger self-energy. Incident kinetic energies (in eV) are marked by arrows on the upper x axis.

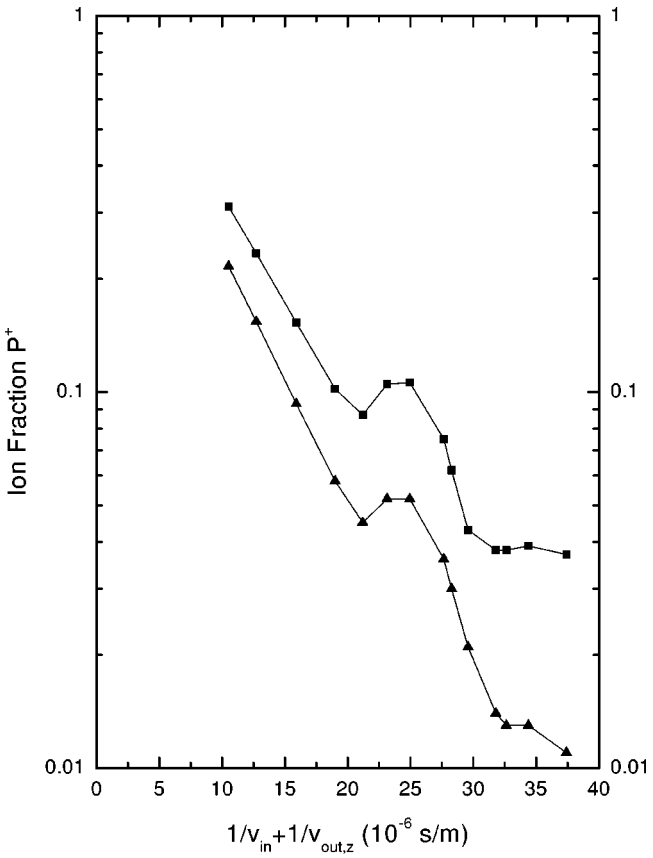

FIG. 5. Comparison of the results of full dynamical calculations of the ion survival probability for a scattering angle of 136°, using *Ansatz* (2) for the Auger self-energies, when these self-energies are calculated using different wave functions for He. Squares: hydrogenlike wave function. Triangles: the Hartree-Fock wave function of Eq. (32).

being zero at the distance of closest approach. This will not affect our results for Auger processes because these processes operate far from the turning point of the trajectory but it may modify the values of our calculated ion fractions since the available time for resonant charge transfer gets longer. However, the main findings of this article are unchanged by this effect.

IV. CONCLUSIONS

We have solved the dynamics of the Newns-Anderson Hamiltonian supplemented with Auger terms (NAA Hamiltonian) and analyzed the case of He^+ scattered from Al. We show that the SCA is a good approximation if the distances between He and Al are larger than around 1 a.u. but that at closer distances this approximation is not reliable due to the strong hybridization between He and the conduction band states of Al. However, one can separate Auger and resonant processes, treating Auger processes within the SCA while keeping the quantum character of resonant processes. We prove that the promotion of the He-1s level due to its interaction with the core levels of Al is an adiabatic process and therefore one can understand charge transfer between He and Al as resonant or Auger exchange of electrons between this promoted orbital and the conduction band states of Al. Agreement between theory and experiment improves considerably if we improve our treatment of the He-1s wave function when calculating the contribution of Auger processes to charge exchange.

ACKNOWLEDGMENTS

We are indebted to F. Flores for many fruitful discussions and for a critical reading of the manuscript. This work has been founded by the spanish Comisión Interministerial de Ciencia y Tecnología under Contract No. BFM-2001-0150. Evelina A. García and N. P. Wang acknowledge the Spanish Comisión Interministerial de Ciencia y Tecnología for financial support. Evelina A. García was also supported by Consejo Nacional de Investigaciones Científicas y Técnicas (CONICET, Argentina) and Fundación Antorchas (Argentina) under Contract No. A-13564/1-26.

*Permanent address: Instituto de Desarrollo Tecnológico para la Industria Química (CONICET-UNL), Güemes 3450, CC91, 3000, Santa Fe, Argentina.
†On leave from Fudan University, Sanghai, People's Republic of China.

[1] A. Blandin, A. Nourtier, and D. W. Hone, J. Phys. (Paris) **37**, 369 (1976).
[2] R. Brako and D. M. Newns, Surf. Sci. **108**, 253 (1981).
[3] J. J. C. Geerlings and J. Los, Phys. Rep. **190**, 133 (1990).
[4] J. J. C. Geerlings, J. Los, J. P. Gauyacq, and N. M. Temme, Surf. Sci. **172**, 257 (1986).
[5] D. C. Langreth and P. Nordlander, Phys. Rev. B **43**, 2541 (1991).
[6] H. Shao, D. C. Langreth, and P. Nordlander, Phys. Rev. B **49**, 13929 (1994).
[7] Evelina A. García, E. C. Goldberg, and M. C. G. Passeggi, Surf. Sci. **325**, 311 (1995); Evelina A. García, P. G. Bolcatto, and E. C. Goldberg, Phys. Rev. B **52**, 16924 (1995).
[8] A. v. Onufriev and J. B. Marston, Phys. Rev. B **53**, 13 340 (1996).
[9] J. Merino and J. B. Marston, Phys. Rev. B **58**, 6982 (1998).
[10] H. D. Hagstrum, Phys. Rev. **96**, 336 (1954).
[11] L. V. Keldysh, Zh. Éksp. Teor. Fiz. **47**, 1515 (1964) [Sov. Phys. JETP **20**, 1018 (1965)].
[12] M. A. Vicente Alvarez, V. H. Ponce, and E. C. Goldberg, Phys. Rev. B **57**, 14919 (1998).
[13] A. G. Borisov, D. Teillet-Billy, and J.-P. Gauyacq, Phys. Rev. Lett. **68**, 2842 (1992).
[14] G. E. Makhmetov, A. G. Borisov, D. Teillet-Billy, and J.-P. Gauyacq, Surf. Sci. **339**, 182 (1995).
[15] P. Nordlander and J. C. Tully, Phys. Rev. Lett. **61**, 990 (1988).
[16] S. A. Deutcher, X. Yang, and J. Burgdörfer, Phys. Rev. A **55**, 466 (1997).
[17] A. G. Borisov, D. Teillet-Billy, and J.-P. Gauyacq, Nucl. Instrum. Methods Phys. Res. B **78**, 49 (1993).
[18] P. Kurpick, U. Thumm, and U. Wille, Phys. Rev. A **56**, 543 (1997).
[19] A. C. Hewson, *The Kondo Problem to Heavy Fermions* (Cambridge University Press, New York, 1993).
[20] R. Monreal and N. Lorente, Phys. Rev. B **52**, 4760 (1995).
[21] W. More, J. Merino, R. Monreal, P. Pou, and F. Flores, Phys. Rev. B **58**, 7385 (1998).
[22] N. P. Wang, Evelina A. García, R. Monreal, F. Flores, E. C. Goldberg, H. H. Brongersma, and P. Bauer, Phys. Rev. A **64**, 012901 (2001).
[23] E. Clementi and C. Roetti, At. Data Nucl. Data Tables **14**, 177 (1974).
[24] N. Lorente and R. Monreal, Phys. Rev. B **53**, 9622 (1996); N. Lorente and R. Monreal, Surf. Sci. **370**, 324 (1997).
[25] P. M. Echenique, F. Flores, and R. H. Ritchie, in *Solid State Physics: Advances in Research and Applications*, edited by H. Ehrenreich and D. Turnbull (Academic, New York, 1990), Vol. 43, p. 229.
[26] R. A. Baragiola and C. A. Dukes, Phys. Rev. Lett. **76**, 2547 (1996).
[27] J. Merino, N. Lorente, P. Pou, and F. Flores, Phys. Rev. B **54**, 10959 (1996).
[28] Evelina A. García and R. Monreal, Phys. Rev. B **61**, 13565 (2000).
[29] E. C. Goldberg, R. Monreal, F. Flores, H. H. Brongersma, and P. Bauer, Surf. Sci. **440**, L875 (1999).
[30] M. A. Cazalilla, N. Lorente, R. Diez Muiño, J.-P. Gauyacq, D. Teillet-Billy, and P. M. Echenique, Phys. Rev. B **58**, 13991 (1998).
[31] B. H. Bransden and C. J. Joaquim, *Physics of Atoms and Molecules* (Longmans, New York, 1980)